DESY 10-029
Edinburgh 2010/06
LTH 867
March 2010

Tuning the strange quark mass in lattice simulations

W. Bietenholz[a], V. Bornyakov[b], N. Cundy[c], M. Göckeler[c], R. Horsley[d], A. D. Kennedy[d], W. G. Lockhart[e], Y. Nakamura[c], H. Perlt[f], D. Pleiter[g], P. E. L. Rakow[e], A. Schäfer[c], G. Schierholz[ch], A. Schiller[f], H. Stüben[i] and J. M. Zanotti[d]

– QCDSF-UKQCD Collaboration –

[a] Instituto de Ciencias Nucleares, Universidad Autónoma de México, A.P. 70-543, C.P. 04510 Distrito Federal, Mexico

[b] Institute for High Energy Physics, 142281 Protovino, Russia and Institute of Theoretical and Experimental Physics, 117259 Moscow, Russia

[c] Institut für Theoretische Physik, Universität Regensburg, 93040 Regensburg, Germany

[d] School of Physics and Astronomy, University of Edinburgh, Edinburgh EH9 3JZ, UK

[e] Theoretical Physics Division, Department of Mathematical Sciences, University of Liverpool, Liverpool L69 3BX, UK

[f] Institut für Theoretische Physik, Universität Leipzig, 04109 Leipzig, Germany

[g] John von Neumann Institute NIC / DESY Zeuthen, 15738 Zeuthen, Germany

[h] Deutsches Elektronen-Synchrotron DESY, 22603 Hamburg, Germany

[i] Konrad-Zuse-Zentrum für Informationstechnik Berlin, 14195 Berlin, Germany

March 4, 2010

Abstract

QCD lattice simulations with $2 + 1$ flavours typically start at rather large up-down and strange quark masses and extrapolate first the strange quark mass to its physical value and then the up-down quark mass. An alternative method of tuning the quark masses is discussed here in which the singlet quark mass is kept fixed, which ensures that the kaon always has mass less than the physical kaon mass. It can also take into account the different renormalisations (for singlet and non-singlet quark masses) occurring for non-chirally invariant lattice fermions and so allows a smooth extrapolation to the physical quark masses. This procedure enables a wide range of quark masses to be probed, including the case with a heavy up-down quark mass and light strange quark mass. Results show the correct order for the baryon octet and decuplet spectrum and an extrapolation to the physical pion mass gives mass values to within a few percent of their experimental values.

1 Introduction

There has been a steady progression of lattice results from a quenched sea to a two-flavour and more recently $2+1$ flavour sea in an attempt to provide a more complete and quantitative description of hadronic phenomena. (By $2+1$ flavours we mean here two mass degenerate up-down, m_l^R, quarks and one strange, m_s^R, quark.) In this letter we discuss some ways of approaching in the m_l^R–m_s^R plane the physical point (m_l^{R*}, m_s^{R*}), where the natural starting point for these paths is an $SU(3)$ flavour symmetric point $m_l^R = m_s^R = m_{sym}^{R(0)}$. (The superscripts *, $^{(0)}$ denote the physical point and flavour symmetric point respectively and ^{R} means the renormalised quantity.) The usual procedure is to estimate the physical strange quark mass and then try to keep it fixed, i.e. $m_s^R = \text{constant}$, as the light quark mass is reduced to its physical value. However the problem is that the kaon mass is always larger than its physical value. We propose here instead to choose the path such that the singlet quark mass is kept fixed,

$$\overline{m}^R = \tfrac{1}{3}(2m_l^R + m_s^R) = \text{constant}\,. \tag{1}$$

This procedure has the advantage that we can vary both quark masses over a wide range, and is thus particularly useful for strange quark physics. $SU(3)_F$ chiral perturbation theory should work well, because both the kaon and η are lighter than their physical values along the entire trajectory. (They both approach their final mass values from below.) Since $SU(3)_F$ chiral perturbation theory is thought to be valid for $m_K < 600\,\text{MeV}$, [1], we should always be able to make use of chiral perturbation theory. If we extend our measurements beyond the symmetric point we can also investigate a world with heavy up-down quarks and a lighter strange quark.

As a 'proof of concept' results given here show firstly the correct order for the baryon octet and decuplet mass spectrum and secondly an extrapolation to the physical pion mass yields results to within a few percent for the baryon masses.

2 Extrapolating flavour singlet quantities

Flavour singlet quantities are flat at a point on the $SU(3)$ flavour symmetric line and hence allow simpler extrapolations to the physical point. This may be shown by considering small changes about a point on the flavour symmetric line. Let $X_S(m_u^R, m_d^R, m_s^R)$ be a flavour singlet object i.e. X_S is invariant under the quark permutation symmetry between u, d and s. So Taylor expanding X_S about a point on the symmetric line where flavour $SU(3)$ holds gives

$$\begin{aligned} & X_S(\overline{m}^{R(0)} + \delta m_l^R, \overline{m}^{R(0)} + \delta m_l^R, \overline{m}^{R(0)} + \delta m_s^R) \\ &= X_{S\,sym}^{(0)} + \left.\frac{\partial X_S}{\partial m_u^R}\right|_{sym}^{(0)} \delta m_l^R + \left.\frac{\partial X_S}{\partial m_d^R}\right|_{sym}^{(0)} \delta m_l^R + \left.\frac{\partial X_S}{\partial m_s^R}\right|_{sym}^{(0)} \delta m_s^R + O((\delta m_q^R)^2)\,. \end{aligned} \tag{2}$$

But on the symmetric line we have

$$\left.\frac{\partial X_S}{\partial m_u^R}\right|_{sym} = \left.\frac{\partial X_S}{\partial m_d^R}\right|_{sym} = \left.\frac{\partial X_S}{\partial m_s^R}\right|_{sym} , \tag{3}$$

and on our chosen trajectory $\overline{m}^R = \text{constant}$,

$$2\delta m_l^R + \delta m_s^R = 0 \,, \tag{4}$$

which together imply that

$$X_S(\overline{m}^{R(0)} + \delta m_l^R, \overline{m}^{R(0)} + \delta m_l^R, \overline{m}^{R(0)} + \delta m_s^R) = X_{S\,sym}^{(0)} + O((\delta m_q^R)^2) \,. \tag{5}$$

In other words, the effect at first order of changing the strange quark mass is cancelled by the change in the light quark mass, so we know that X_S must have a stationary point on the $SU(3)_F$ symmetric line. If we were making a quadratic extrapolation to the physical point, this eliminates a free parameter – we only need two parameters to make the quadratic extrapolation. This is particularly useful for quantities like the force scale, r_0, where we do not have any theoretical input from chiral perturbation theory. Also the fact that X_S is flat at the symmetric point means that the extrapolated value cannot lie very far from the measured value. Other paths are not so fortunate. What we are doing is to keep the flavour singlet part of the quark matrix constant, while increasing the octet part (the changes in quark masses are proportional to λ_8). Gluons are flavour-blind, they cannot couple directly to a flavour octet operator, they can only see flavour singlets – which can only occur in the square of the octet part of the mass. So everything about our gluon configuration will vary quadratically with the distance from the symmetric point. So we are generating all our configurations closer to the physical point by taking the $\overline{m}^R = \text{constant}$ line.

Other potential advantages include: as $m_l^R \searrow m_l^{R*}$ then $m_s^R \nearrow m_s^{R*}$, i.e. , the m_s^R–m_l^R splitting or m_K increases to its physical value. The singlet quark mass is correct from the very beginning; numerically the simulation cost change should be moderate and the update algorithm is expected to equilibrate quickly along this path.

For X_S we have several possibilities: for example the centre of mass squared of the meson octet, $\frac{1}{3}(m_\pi^2 + 2m_K^2)$ or the centre of mass of the baryon octet or decuplet, $X_N = \frac{1}{3}(m_N + m_\Sigma + m_\Xi) = 1.150\,\text{GeV}$, $X_\Delta = \frac{1}{3}(2m_\Delta + m_\Omega) = 1.379\,\text{GeV}$ respectively or a gluonic quantity such as $X_r = 1/r_0$.

We can check the above result, eq. (5), by considering leading order (LO) together with next to leading order (NLO) $SU(3)_F$ chiral perturbation theory, χPT. Note that LO χPT corresponds to linear terms in the expansion of X_S and so from eq. (5) will be absent. Rather than using the full symmetric 1+1+1 results it is sufficient to just consider the $2+1$ results. Let us first define $\chi_q = 2B_q^R m_q^R$

and furthermore set $\chi_\eta = (\chi_l + 2\chi_s)/3$ and $\chi_K = (\chi_l + \chi_s)/2$. Then $\chi_l + \chi_\eta = 2\overline{\chi}$ and $\chi_l + 2\chi_K = 3\overline{\chi}$ are constants on our trajectory and so

$$\delta\chi_l + \delta\chi_\eta = 0 = \delta\chi_l + 2\delta\chi_K \,. \tag{6}$$

This means that any functions of the form

$$f(\chi_\eta) + f(\chi_l) \quad \text{or} \quad 2h(\chi_K) + h(\chi_l) \,, \tag{7}$$

will have zero derivative at the symmetric point, so they are permitted as higher order corrections. Using the LO and NLO results from e.g. [2, 3, 4] (where further details of the functions can be found) we have

$$\begin{aligned}
\tfrac{1}{3}(2m_K^2 + m_\pi^2) &= \overline{\chi} + \{f_\pi(\chi_\eta) + f_\pi(\chi_l)\} \\
\tfrac{1}{3}(m_N + m_\Sigma + m_\Xi) &= m_{0N} + 2(\alpha_N + \beta_N + 3\sigma_N)\overline{\chi} \\
&\quad + \{f_N(\chi_\eta) + f_N(\chi_l) + 2h_N(\chi_K) + h_N(\chi_l)\} \\
\tfrac{1}{3}(2m_\Delta + m_\Omega) &= m_{0\Delta} + 2(\gamma_\Delta - 3\sigma_\Delta)\overline{\chi} \\
&\quad + \{f_\Delta(\chi_\eta) + f_\Delta(\chi_l) + 2h_\Delta(\chi_K) + h_\Delta(\chi_l)\} \,,
\end{aligned} \tag{8}$$

with

$$f_\pi(\chi) = \alpha_\pi \overline{\chi}^2 + \beta_\pi \chi^2 + \gamma_\pi \ln(\chi/\Lambda_\chi) \,, \tag{9}$$

and

$$\begin{aligned}
f_S(\chi) &= \delta_S \chi^{\frac{3}{2}} + \epsilon_S F(\chi^{\frac{1}{2}}) \\
h_S(\chi) &= \zeta_S \chi^{\frac{3}{2}} + \eta_S F(\chi^{\frac{1}{2}}) \,,
\end{aligned} \tag{10}$$

(with $S = N,\ \Delta$). $\alpha,\ \ldots,\ \eta$ are combinations of the low energy constants. The NLO results are shown in curly brackets. These results are thus all in agreement with our previous discussion. Note also that on the $\overline{m}^R$ = constant trajectory some of the low energy constants combine together leading to fits with fewer free parameters.

We now have to relate the known physical point to the initial symmetric point. As discussed above, we expect X_S to be constant (in m_l^R) up to small corrections, so we will find it sufficient to consider only LO χPT. Then keeping $\overline{m}^R$ constant means keeping $(2m_K^2 + m_\pi^2)/3$ constant. For this path choice, we can now relate the known physical point to the initial symmetric point,

$$\left.\frac{\frac{1}{3}(2m_K^2 + m_\pi^2)}{X_S^2}\right|^* = \left.\frac{m_\pi^2}{X_S^2}\right|_{sym}^{(0)} \,, \tag{11}$$

where $S = N,\ \Delta$ and r respectively. So simulations along the flavour symmetric line and using eq. (11) are sufficient to determine the initial point. This procedure is illustrated in Fig. 1 in the next section.

If we now generalise to consider higher order terms from the above discussion lines of constant X_S are curved though they do still have to have the slope of -2 at the point where they cross the $m_l^R = m_s^R \equiv m_{sym}^R$ line. Now we have to specify more closely what we mean when we keep $2m_K^2 + m_\pi^2$ constant, as different scale choices give different paths. As shown above in eq. (5) on our trajectory this is a higher order effect, on other choices of trajectory the difference between different scale definitions would be much more important. If we make different choices of the quantity we keep constant at the experimentally measured physical value, for example the choices discussed above we get slightly different trajectories. The different trajectories begin at slightly different points along the symmetric line. Initially they are all parallel with slope -2, but away from the symmetry line they can curve, and will all meet at the physical point.

3 Clover fermions

The above properties are general; we now apply them to 'clover' or $O(a)$-improved Wilson fermions. There are now some additional points to consider when relating the bare quark mass (which is the input parameter) to the renormalised quark mass. The problem is that for fermions with no chiral symmetry the singlet, S, and non-singlet, NS, quark mass can renormalise differently which means that the relation to the bare quark masses and hence κ, which is the adjustable simulation parameter, is more complicated [5]

$$\begin{aligned} m_q^R &= Z_m^{NS}(m_q - \overline{m}) + Z_m^S \overline{m} \\ &= Z_m^{NS}(m_q + \alpha_Z \overline{m}) \,, \end{aligned} \tag{12}$$

($q = l,\, s$) with $\alpha_Z = (Z_m^S - Z_m^{NS})/Z_m^{NS}$ and bare quark mass defined by

$$am_q = \frac{1}{2}\left(\frac{1}{\kappa_q} - \frac{1}{\kappa_{sym;c}}\right) , \tag{13}$$

where $\kappa_{sym;c}$ is defined by the vanishing of the quark mass along the symmetric line, i.e. for 3 mass degenerate flavours. Now from LO χPT we have

$$\tfrac{1}{3}(2(am_K)^2 + (am_\pi)^2) \propto \tfrac{2}{9}(1 + \alpha_Z) a\overline{m} \,, \tag{14}$$

and so the path $a\overline{m} =$ constant remains as $\frac{1}{3}(2(am_K)^2 + (am_\pi)^2)$ constant. This translates to

$$\kappa_s = \frac{1}{\frac{3}{\kappa_{sym}^{(0)}} - \frac{2}{\kappa_l}} \,, \tag{15}$$

where $\kappa_{sym}^{(0)}$ is the appropriate κ on the $SU(3)$ flavour symmetric line. As discussed previously higher order corrections have zero derivative at the flavour $SU(3)$ symmetric point and so should be small.

$O(a)$-improvement also leads to a change in the coupling constant, $g_0^2 \to \tilde{g}_0^2 = g_0^2(1 + b_g a\overline{m})$, [6, 7]. However for our trajectory as $\overline{m}$ is held constant then $\tilde{g}_0^2$ also remains constant. Also, [7], $\overline{m}^R = Z_m^S\,[1 + (3\overline{d}_m + d_m u(\xi))a\overline{m}]\overline{m}$ where $\overline{d}_m$, d_m are improvement coefficients and $u(\xi) = 3 - 4\xi + 2\xi^2$ with $\xi = m_l/m_{sym}^{(0)}$. As $u(\xi)$ has a minimum at $\xi = 1$, it is again flat at the symmetry point, as expected. We have estimated that with the parameters used below, the correction term in $\overline{m}^R$ remains very small and so we shall ignore this here.

The particular clover action used here consists of the tree level Symanzik improved gluon action together with a mild 'stout' smeared fermion action. Further details, [8, 9], and a determination of the non-perturbative, NP, coefficient used for the clover term are described in [9]. Simulations have been performed using the Hybrid Monte Carlo, HMC, algorithm with mass preconditioning for 2 mass-degenerate flavours and the rational HMC, [10] for the 1-flavour. Two programmes were used, a Fortran programme, [11], and also the Chroma programme, [12]. All the runs described here are on $24^3 \times 48$ lattices at $\beta = 5.50$, $c_{sw} = 2.65$, [9] (we describe the determination of the scale later). We first need to determine the symmetric point, using eq. (11).

A series of runs on the $SU(3)$ flavour symmetric line gives an estimate of our starting value $\kappa_{sym}^{(0)}$. Some are shown in Fig. 1 (where we plot $(2m_K^2 - m_\pi^2)/X_S^2$ against m_π^2/X_S^2 using the scales X_S with $S = N$, Δ and r) as the points lying on the $y = x \equiv m_\pi^2/X_S^2$, black dashed line. We seek the point on the symmetric line where eq. (11) holds. This gives an estimate for $\kappa_{sym}^{(0)}$. We find $\kappa_{sym}^{(0)} = 0.12090$ which we shall take as our starting value.

From this we can now, given a κ_l, find the corresponding κ_s using eq. (15). After some experimentation we chose the κ_l, κ_s values given in Table 1. Note

κ_l	κ_s	
0.12083	0.12104	$m_l > m_s$
0.12090	0.12090	$m_l = m_s$
0.12095	0.12080	$m_l < m_s$
0.12100	0.12070	$m_l < m_s$
0.12104	0.12062	$m_l < m_s$

Table 1: (κ_l, κ_s) values simulated on $24^3 \times 48$ lattices.

that it is possible to choose κ_l, κ_s values (here $(0.12083, 0.12104)$) such that $m_l > m_s$. In this strange world, as previously mentioned, we would expect to see an *inversion* of the particle spectrum, with for example the nucleon being the heaviest octet particle.

These results[1] are also shown in Fig. 1. Each data set comprises $\sim O(2000)$ trajectories. (Note that our lowest pion mass has $m_\pi L \sim 3.4$ and may be showing

[1]Preliminary results were given in [13].

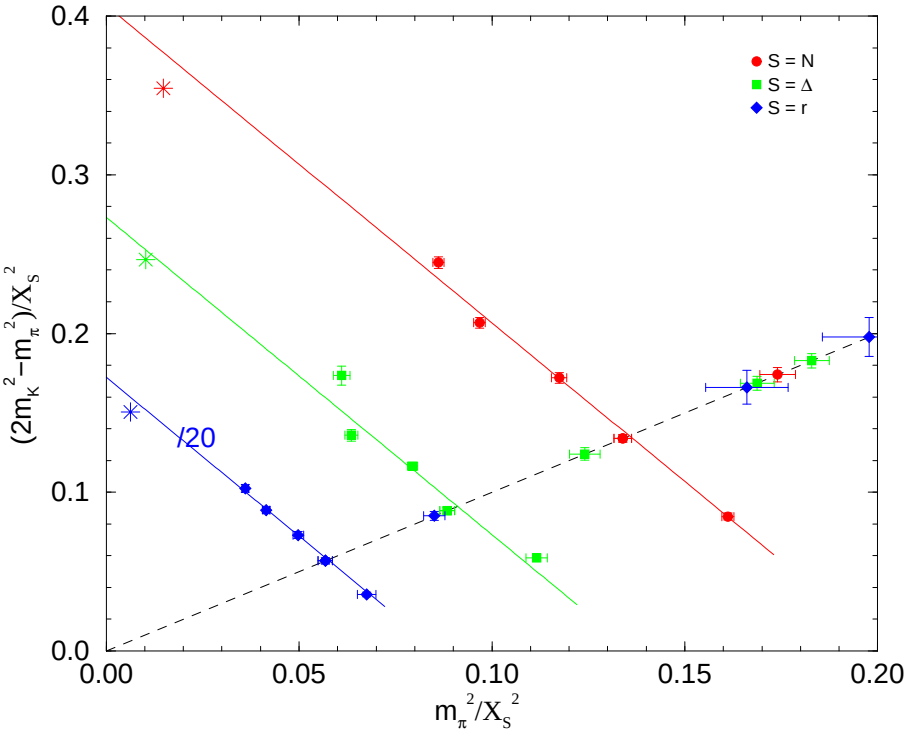

Figure 1: $(2m_K^2 - m_\pi^2)/X_S^2$ (y-axis) against m_π^2/X_S^2 (x-axis) using $S = N$ (red circles) $S = \Delta$ (green squares) and $S = r$ (blue diamonds). The $SU(3)$ flavour symmetric line ($y = x$) is the dashed line. (For convenience the results for $S = r$ have been divided by a factor of 20.) The experimental points using the three singlet quantities, X_S, $S = N$, Δ, r are shown as stars. The solid lines are fits using eq. (16).

some sign of finite size effects.) Also shown is a fit to constant $2m_K^2 + m_\pi^2$ by

$$\frac{2m_K^2 - m_\pi^2}{X_S^2} = c_S - 2\,\frac{m_\pi^2}{X_S^2}\,. \tag{16}$$

The numerically simulated points all lie (approximately) on the line of constant $2m_K^2 + m_\pi^2$. There is also consistency between the various singlet quantities used.

To determine the scale we again use the constancy of X_S. In Fig. 2 we show aX_S against $(am_\pi)^2$ for $S = N$, Δ, r together with constant fits. (Although the physical limit is also shown, as we are making a constant fit, this is not important here.) Then from $aX_S =$ constant we can determine the scale giving $a = 0.083\,\text{fm}$, $0.084\,\text{fm}$ for $S = N$, Δ respectively. We use in future the $S = N$ or $a = 0.083\,\text{fm}$ value. This means that the box size, $L \sim 2\text{fm}$. While for $X = r$ the numerical results are the flattest, the physical value is less well known. However reversing the argument and using $a = 0.083\,\text{fm}$ gives $r_0 = 0.50\,\text{fm}$.

As is apparent from Fig. 1, we have slightly underestimated $\kappa^{(0)}_{sym}$ (reflected by the fact that $\frac{1}{3}c_S$ from eq. (16) is not quite equal to $\frac{1}{3}(2m_K^2 + m_\pi^2)/X_S^2|^*$, cf

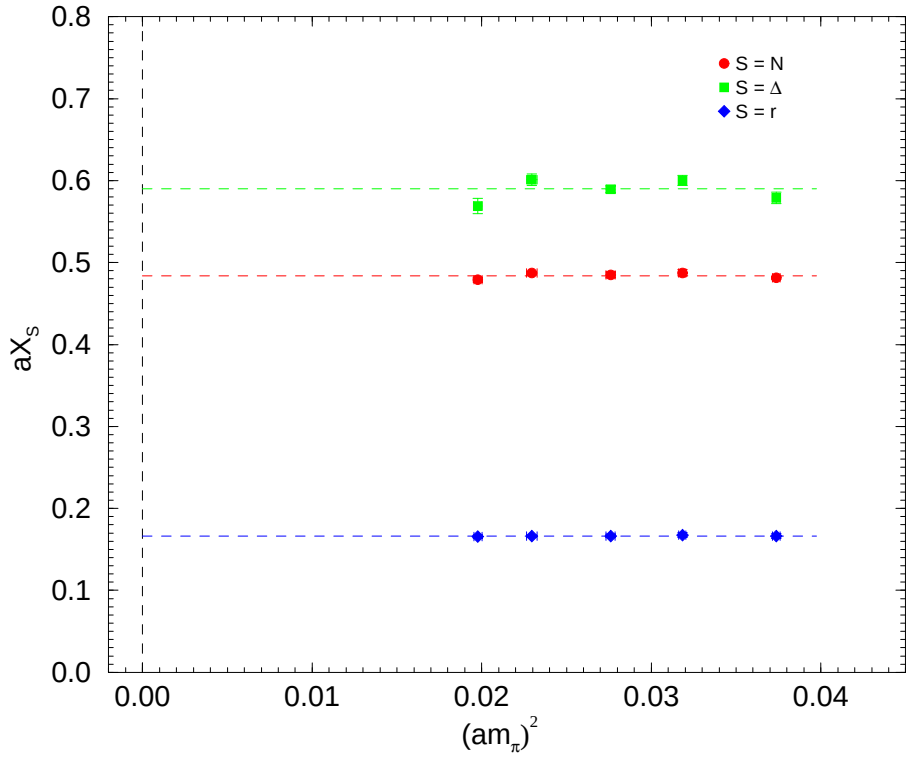

Figure 2: aX_S against $(am_\pi)^2$ for $S = N$ (red circles) $S = \Delta$ (green squares) and $S = r$ (blue diamonds). Constant fits are also shown (dashed lines).

eq. (11)). We can estimate the significance of this on the kaon mass, by taking the value of $(2m_K^2 - m_\pi^2)/X_N^2$ at the physical pion mass, $(m_\pi^2/X_N^2)|^*$ in the figure. This gives $m_K \sim 509\,\mathrm{MeV}$, a $\sim 3\%$ discrepancy when compared to the experimental kaon mass of $\sim 494\,\mathrm{MeV}$.

4 Hadron spectrum

The octet (and decuplet) baryon masses are degenerate at the $SU(3)$ flavour symmetric point and then fan out. As a first example we now give some mass results in Fig. 3 for the baryon octet: N, Λ, Σ, Ξ, together with a constrained fit from LO χPT, e.g. [3] about the $SU(3)$ flavour symmetric point,

$$\begin{aligned} m_N &= A_N + 2(\alpha_N + \beta_N)(m_\pi^2 - m_\pi^2|^{(0)}_{sym}) \\ m_\Sigma &= A_N + (\alpha_N - 2\beta_N)(m_\pi^2 - m_\pi^2|^{(0)}_{sym}) \\ m_\Lambda &= A_N - (\alpha_N - 2\beta_N)(m_\pi^2 - m_\pi^2|^{(0)}_{sym}) \\ m_\Xi &= A_N - 3\alpha_N(m_\pi^2 - m_\pi^2|^{(0)}_{sym})\,, \end{aligned} \tag{17}$$

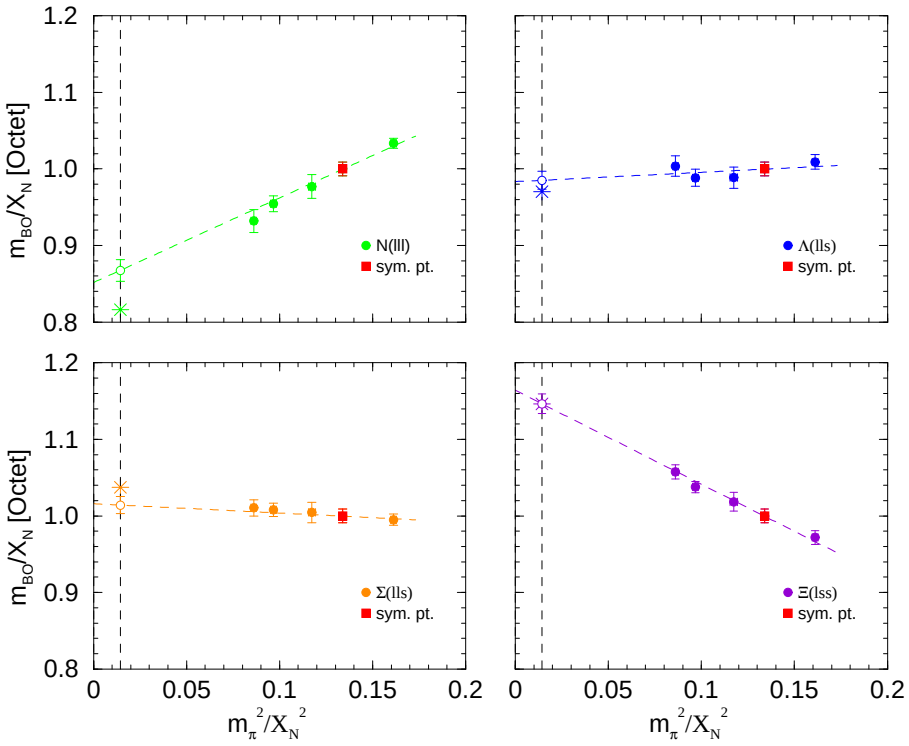

Figure 3: The octet baryon masses O where $O = N$, Λ, Σ and Ξ using the scale $S = N$, upper left to lower right respectively, together with the fit from eq. (17). The common $SU(3)_F$ symmetric quark mass value is shown in red. The experimental values are shown with stars.

where $A_N \equiv m_{0N} + 2(\alpha_N + \beta_N + 3\sigma_N)\overline{m}$, α_N, β_N are the three fit parameters (in the figure we have also normalised the masses with X_N). Similarly in Fig. 4 results are given for the baryon decuplet: Δ, Σ^*, Ξ^*, Ω, again together with the constrained fit from LO χPT, e.g. [4],

$$\begin{aligned} m_\Delta &= A_\Delta + 2\gamma_\Delta(m_\pi^2 - m_\pi^2|^{(0)}_{sym}) \\ m_{\Sigma^*} &= A_\Delta \\ m_{\Xi^*} &= A_\Delta - 2\gamma_\Delta(m_\pi^2 - m_\pi^2|^{(0)}_{sym}) \\ m_\Omega &= A_\Delta - 4\gamma_\Delta(m_\pi^2 - m_\pi^2|^{(0)}_{sym})\,, \end{aligned} \tag{18}$$

where $A_\Delta \equiv m_{0\Delta} + 2(\gamma_\Delta - 3\sigma_\Delta)\overline{m}$, γ_Δ are the two fit parameters.

Both these figures illustrate the 'proof of concept' of the method described here. The correct ordering of the particle spectrum has been achieved (including the anti-ordering behind the symmetric point). The masses (using the scale determined by $S = N$) are given in Table 2. The results are already within a few percent of their experimental values, and clearly show that higher orders of χPT are small. We can expect an improvement for results closer to the physical pion mass.

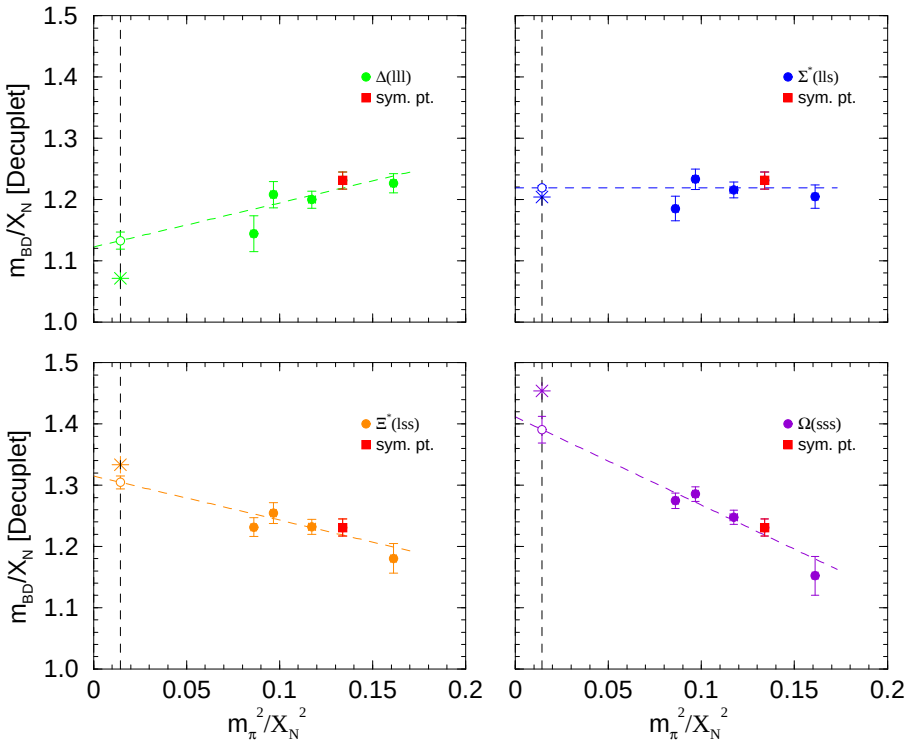

Figure 4: The decuplet baryon masses, D, where $D = \Delta$, Σ^*, Ξ^* and Ω (also using the scale $S = N$), together with the fit from eq. (18). The common $SU(3)_F$ symmetric quark mass value is shown in red. The experimental values are shown with stars.

Finally to illustrate better the 'fanning' out of the results we show in Fig. 5 mass splittings for the baryon octet: $m_N - m_\Sigma$, $m_\Lambda - m_\Sigma$, $m_\Xi - m_\Sigma$ together with the constrained fit from eq. (17). Considering mass splittings has the advantage that the results can be obtained directly from the ratio of correlation functions, which leads to a significant reduction in the error.

5 Conclusions

We have suggested here that the simplest way of approaching the physical point in lattice simulations is to hold the singlet quark mass fixed from a point on the $SU(3)$ flavour symmetric line. This has been shown both theoretically and numerically (using an NP $O(a)$-improved $2+1$ flavour clover action) to lead to very smooth results in the extrapolation of singlet quantities to the physical pion mass. Exploratory results for the hadron mass spectrum give masses in the correct order (including *inversion* when $m_l > m_s$ i.e. we can simulate a strange world where, for example, the nucleon can decay). Furthermore the extrapolated masses for both the baryon octet and decuplet are within a few

Particle	Expt. [MeV]	Result [MeV]	Discrep.
m_N	939	998(16)	6%
m_Λ	1116	1133(14)	2%
m_Σ	1193	1166(13)	2%
m_Ξ	1318	1318(15)	0%
m_Δ	1232	1303(16)	5%
m_{Σ^*}	1385	1402(05)	1%
m_{Ξ^*}	1533	1501(12)	2%
m_Ω	1673	1599(25)	4%

Table 2: Masses for the baryon octet and decuplet.

percent of their experimental values. To improve the situation further clearly we need simulations closer to the physical pion mass. At present in our simulations the pion mass decreases from $\sim 450\,\mathrm{MeV}$ to $\sim 335\,\mathrm{MeV}$ while the kaon mass increases from $\sim 400\,\mathrm{MeV}$ to $\sim 450\,\mathrm{MeV}$, (experimentally $m_\pi = 138\,\mathrm{MeV}$, $m_K = 494\,\mathrm{MeV}$). Also to improve the accuracy of the approach to the physical pion mass another line of constant singlet mass should be found, which will allow interpolation/extrapolation around the physical pion mass. Finally we note that even LO χPT seems to be working very well around the flavour symmetric point. Further results will be published elsewhere, [14].

Acknowledgements

The numerical calculations have been performed on the IBM BlueGeneL at EPCC (Edinburgh, UK), the BlueGeneL and P at NIC (Jülich, Germany), the SGI ICE 8200 at HLRN (Berlin-Hannover, Germany) and the JSCC (Moscow, Russia). We thank all institutions. The BlueGene codes were optimised using Bagel, [15]. This work has been supported in part by the EU Integrated Infrastructure Initiative *Hadron Physics* and by the DFG under contract SFB/TR 55 (Hadron Physics from Lattice QCD).

References

[1] H. Leutwyler, private communication.

[2] C. Allton, D. J. Antonio, Y. Aoki, T. Blum, P. A. Boyle, N. H. Christ, S. D. Cohen, M. A. Clark, C. Dawson, M. A. Donnellan, J. M. Flynn, A. Hart, T. Izubuchi, A. Jüttner, C. Jung, A. D. Kennedy, R. D. Kenway, M. Li, S. Li, M. F. Lin, R. D. Mawhinney, C. M. Maynard, S. Ohta, B. J. Pendleton, C. T.

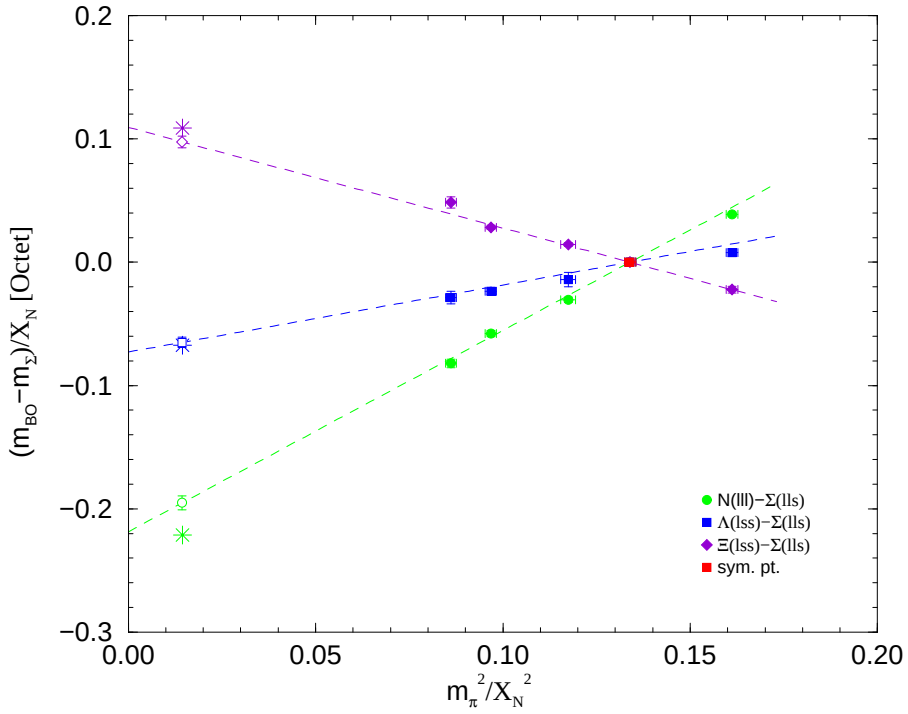

Figure 5: The octet baryon mass splittings $O - \Sigma$ where $O = N$, Λ and Ξ using the scale $S = N$. The common $SU(3)_F$ symmetric quark mass value is shown in red. The experimental values are shown with stars.

Sachrajda, S. Sasaki, E. E. Scholz, A. Soni, R. J. Tweedie, J. Wennekers, T. Yamazaki and J.M. Zanotti (RBC-UKQCD Collaborations), *Phys. Rev.* **D78**, 114509 (2008), [arXiv:0804.0473[hep-lat]].

[3] A. Walker-Loud, *Nucl. Phys.* **A747** (2005) 476, [arXiv:hep-lat/0405007].

[4] B. C. Tiburzi and A. Walker-Loud, *Nucl. Phys.* **A748** (2005) 513, [arXiv:hep-lat/0407030].

[5] M. Göckeler, R. Horsley, A. C. Irving, D. Pleiter, P. E. L. Rakow, G. Schierholz and H. Stüben (QCDSF-UKQCD Collaborations) *Phys. Lett.* **B639** (2006) 307, [arXiv:hep-ph/0409312]; P. E. L. Rakow, *Nucl. Phys. Proc. Suppl.* **140** (2005) 34, [arXiv:hep-lat/0411036].

[6] M. Lüscher, S. Sint, R. Sommer and P. Weisz, *Nucl. Phys.* **B478** (1996) 365, [arXiv:hep-lat/9605038].

[7] T. Bhattacharya, R. Gupta, W. Lee, S. R. Sharpe and J. M. S. Wu, *Phys. Rev.* **D73** (2006) 034504, [arXiv:hep-lat/0511014].

[8] R. Horsley, H. Perlt, P. E. L. Rakow, G. Schierholz and A. Schiller, *Phys. Rev.* **D78** (2008) 054504, [arXiv:0807.0345].

[9] N. Cundy, M. Göckeler, R. Horsley, T. Kaltenbrunner, A. D. Kennedy, Y. Nakamura, H. Perlt, D. Pleiter, P. E. L. Rakow, A. Schäfer, G. Schierholz, A. Schiller, H. Stüben and J. M. Zanotti (QCDSF-UKQCD Collaborations), *Phys. Rev.* **D79** (2009) 094507, [arXiv:0901.3302[hep-lat]].

[10] M. A. Clark and A. D. Kennedy, *Phys. Rev. Lett.* **98** (2007) 051601, [arXiv:hep-lat/0608015].

[11] M. Göckeler, R. Horsley, Y. Nakamura, H. Perlt, D. Pleiter, P. E. L. Rakow, G. Schierholz, A. Schiller, T. Streuer, H. Stüben and J. M. Zanotti (QCDSF Collaboration), *PoS(LATTICE2007)* **041**, (2007) [arXiv:0712.3525 [hep-lat]].

[12] R. Edwards and B. Joó, *Nucl. Phys. Proc. Suppl.* **140** (2005) 832, [arXiv:hep-lat/0409003].

[13] W. Bietenholz, V. Bornyakov, N. Cundy, M. Göckeler, R. Horsley, A. D. Kennedy, Y. Nakamura, H. Perlt, D. Pleiter, P. E. L. Rakow, A. Schäfer, G. Schierholz, A. Schiller, H. Stüben and J. M. Zanotti, *PoS(LAT2009)* **102**, (2009) [arXiv:0910.2963 [hep-lat]].

[14] W. Bietenholz *et al.* (QCDSF–UKQCD Collaborations), in preparation.

[15] P. A. Boyle, http://www.ph.ed.ac.uk/∼paboyle/Bagel.html (2005).